

Practical Decision Making Based on Joint Geometric-Probabilistic Analysis

Mostafa Borhani

*Dept. of Electrical & Computer Engineering, Tarbiat Modares University, IAU of Mahdishahr, IRIB Technical Research Institute, m_borhani@irib.ir
m.borhani@modares.ac.ir*

Abstract: This article gives an outline of the novel scheme for increasing performance of object recognition based on approximation of high-resolution wavelet coefficients with morphological deformation operators. The affectivity of statistical pre-processing techniques such as morphological boundary extraction is excavated. The dependency between parent and child wavelet coefficients of natural images was exploited by a generalized Bayesian-based algorithm. The basic idea is to choose upper bands wavelet coefficients between transform outputs of original and morphological presentation of image. It can be applied without any prior knowledge about probability distributions of wavelet coefficients. This is the simplest way to use novel scheme. In other way, the problem can be considered as the estimation of high resolution wavelet coefficients using a priori probability distribution with Bayesian estimation techniques, such as the maximum a posterior (MAP) estimator.

Keywords: Object Recognition; Morphological operators; Wavelet decomposition; Image enhancement; Edge detection; Image processing.

I. INTRODUCTION

Mathematical morphological image processing [1] as a powerful geometric image analysis technique finds many applications in object matching and pattern recognition. Discontinuous object boundaries especially in noisy images can be avoided by applying morphological algorithms to connect edges. Morphological contour grouping techniques such as edge linking [2] were concentrated mainly on extracting salient curves [3]. Their improvements [4] favor closed objects rather than long and smooth shapes. Methods based on active contours can be employed to detect objects whose boundaries are either smooth or not necessarily defined by gradients [5].

Wavelets mathematical tools and methodologies are nowadays widely used in a variety of science fields by providing simultaneous time and frequency information. The fact that the wavelets are effectively localized in space and frequency (Heisenberg's uncertainty principle) results more advantageous in many applications; such as pattern reorganization, object detection and de-noising.

Statistical models of wavelet coefficients of natural images [6,7,8] have emerged as a powerful tool for wavelets based object detection especially which exploit the dependence between coefficients give better results compared to the ones using an independent assumption [9, 10, 11,12]. Univariate distribution models (such as the G. Laplacian [13,14], γ -stable [15,16], exponential [17], Bessel K Form [18,19,20] and

mixture [21,22] distributions) and multivariate (MV) models (such as the MV Laplacian [9], MV exponential [23], MV γ -stable [10], MV Bessel K Form [18], MV scale mixture of Gaussian [11], MV normal inverse Gaussian [24], and MV Elliptically Contoured Distribution (ECD) [25] distributions) mostly assume independency of natural image wavelet coefficients [19,20] but in some applications their forms are not effectively functional [26]. Based on various prior models such as those mentioned above, many estimators can be developed. This work characterizes bivariate estimators considering the parent and children relationship of wavelet coefficients of natural images for heavy tailed distributions [9].

This paper develops a shape detection method based on combining wavelet coefficients of both the original and morphologically filtered image for vision applications. The author designed a shape-based image processing and examined it over several approaches. This method can be generalized to many shape recognition algorithms. Experimental results show that the novel detection plan can achieve more accurate recognition performance. This improvement was achieved by applying an advanced pre-processing algorithm.

The overall structure of the paper is organized as follows. The section II is a review of the pre-processing block and its affectivity in object detection. In section III, the novel scheme for approximation of high-resolution wavelet coefficients was explicitly shown in detail. The experimental results and discussions are given in section IV. Some concluding remarks presented in section V.

II. MORPHOLOGICAL BOUNDARY EXTRACTION

Morphological image filtering is a powerful nonlinear object detection pre-processing block. The techniques of mathematical morphology are simple and efficient, especially in curve representation of segmented object and boundary detection. Dilation (1), erosion (2), opening (3) and closing (4) in binary and gray-level images (5-8) in median, rank, and stack filters can be used for image smoothing or simplification, noise suppression and edge or contrast enhancement. Figure 1 demonstrates the proposed scheme for object detection based on statistical pre-processing techniques.

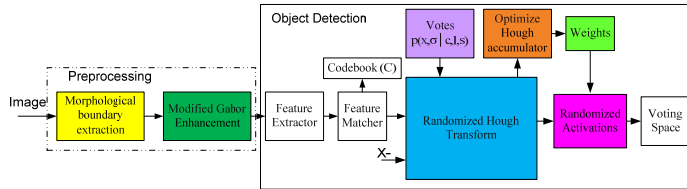


Figure 1. The proposed scheme for object detection.

The top-hat transformation [27] can detect bright blobs and the valley detector can be used to detect dark blobs. The morphological peak (9) / valley (10) detectors can be applied in situations where the peaks or valleys are not intelligibly distinguished from their surroundings.

Morphological-rank-linear (MRL) method as a general class of nonlinear systems is a powerful tool for image processing and a combination of a morphological-rank filter and a linear Finite Impulse Response (FIR) filter. Pessoa and Maragos [27] developed an adaptive optimal design of MRL filters based on the steepest descent method. MRL filters have wide applications such as pattern recognition [27], boundary detection [28], image enhancement and feature detection [29] and Gaussian curvature based shape representation [30].

- X : Object
- B : Windows set
- \vee : Supremum
- \wedge : Infimum

$$X \oplus B = \{x + y : x \in X, y \in B\} = \bigcup_{y \in B} \{x + y : x \in X\} \quad (1)$$

$$X \ominus B = \{x - y : x \in X, y \in B\} = \bigcup_{y \in B} \{x - y : x \in X\} \quad (2)$$

$$X \odot B \equiv (X \ominus B) \oplus B \quad (3)$$

$$X \otimes B \equiv (X \oplus B) \ominus B \quad (4)$$

$$(f \oplus B)(x) \equiv \vee_{y \in B} f(x - y) \quad (5)$$

$$(f \ominus B)(x) \equiv \wedge_{y \in B} f(x + y) \quad (6)$$

$$f \odot B \equiv (f \ominus B) \oplus B \quad (7)$$

$$f \otimes B \equiv (f \oplus B) \ominus B \quad (8)$$

$$\text{Peak}(f) = f - f \odot B \quad (9)$$

$$\text{Valley}(f) = f \otimes B - f \quad (10)$$

Its basic operations, opening and closing, have translation invariance, monotony, duality and idempotent [31]. These essential properties lead to various applications for open-close

filters [32] such as image smoothing, image segmentation and corner and edge detection. There are several edge detection techniques using morphology such as erosion residue, dilation residue, morphological gradient and reduced noise morphological gradient edge detector.

The morphological gradient edge detection method, based on eroded and dilated image, provides good edge detection and can be expressed as

$$E_G(A) = (A \oplus B) - (A \ominus B) \quad (11)$$

The reduced noise morphological edge detection [28] algorithm, used to pre-process image filtering noise, can be formulated as

$$E_{\text{Reduced-noise}}(A) = M \oplus B - M \text{ where } M = ((A \otimes B) \odot B) \otimes B \quad (12)$$

Some other very well-known edge detection algorithms based on directional gradients include Prewitt, Sobel and Roberts Cross. Their convolution kernels are displaced as Figure 2 and their gradient magnitude is given by $G = \sqrt{G_x^2 + G_y^2}$ and it can be approximated as $G \approx |G_x| + |G_y|$.

Convolution kernel	G_x	G_y
Sobel	$\begin{bmatrix} -1 & 0 & 1 \\ -2 & 0 & 2 \\ -1 & 0 & 1 \end{bmatrix}$	$\begin{bmatrix} 1 & 2 & 1 \\ 0 & 0 & 0 \\ -1 & -2 & -1 \end{bmatrix}$
Prewitt	$\begin{bmatrix} -1 & 0 & 1 \\ -1 & 0 & 1 \\ -1 & 0 & 1 \end{bmatrix}$	$\begin{bmatrix} 1 & 1 & 1 \\ 0 & 0 & 0 \\ -1 & -1 & -1 \end{bmatrix}$
Roberts Cross	$\begin{bmatrix} 1 & 0 \\ 0 & -1 \end{bmatrix}$	$\begin{bmatrix} 0 & 1 \\ 1 & 0 \end{bmatrix}$

Figure 2. The various convolution kernel.

The canny edge detection algorithm is more complex than Sobel, Prewitt and morphological gradient. It include six step process such as noise removal, finding edge strengths with Sobel operator, computing edge directions, discretizing edge directions, non-maxima suppression and hysteresis.

In this paper a pseudo Gaussian mask was applied to perform edge detection in real-time such as Figure 3.

$$\text{Pseudo Gaussian mask } G(x, y) = \frac{1}{2\pi\sigma^2} e^{-\frac{x^2+y^2}{2\sigma^2}} \quad (13)$$

The proposed convolution kernel for shape matching is a $k \times k$ smoothing kernel (5*5) to reduce noise and smooth input image shown in Figure 4.

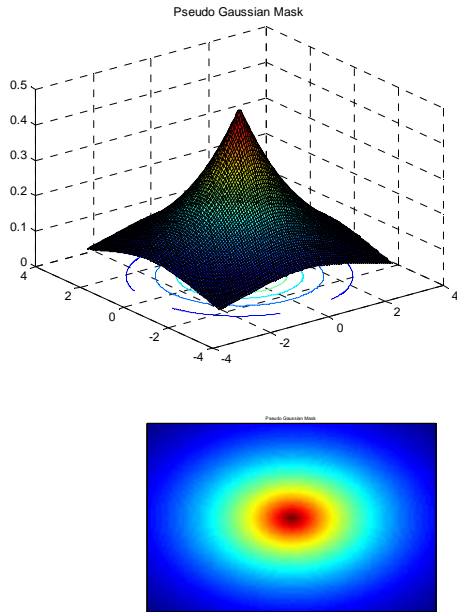


Figure 3. The Pseudo Gaussian mask convolution kernel.

Convolution kernel	=
Novel	-1 -1 -1 -1 -1
	-1 0 0 0 -1
	-1 0 2 0 -1
	-1 0 0 0 -1
	-1 -1 -1 -1 -1

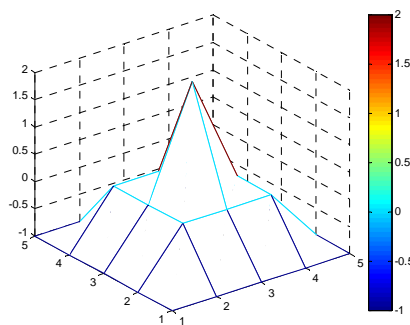
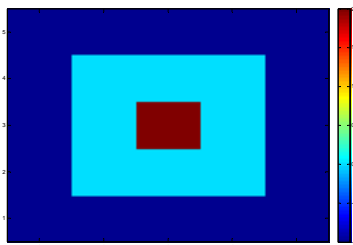


Figure 4. The proposed convolution kernel for shape matching.

III. NOVEL PRE-PROCESSING SCHEME

In this novel scheme, a combination of shape-based image processing operations and wavelet representation is introduced to improve the performance of the algorithms for object detection. The original image is processed with morphological operators to approximate high-resolution wavelet coefficients. Boundary detection property of morphological operations was well mentioned by [28,33]. This paper provides a new object recognition scheme based on wavelet decomposition of both the original and morphologically-filtered image. A schematic diagram of the proposed algorithm is demonstrated in Figure 5. Table I summarized MAP decision rules for various probability distributions of wavelet coefficients [9], where $W = [w_1, w_2]$ is wavelet coefficient, w_2 represent the parent of w_1 . w_1 and w_2 are uncorrelated but not independent, is the normalization constant, "O" index was denoted as Original image and "M" was used for Morphology.

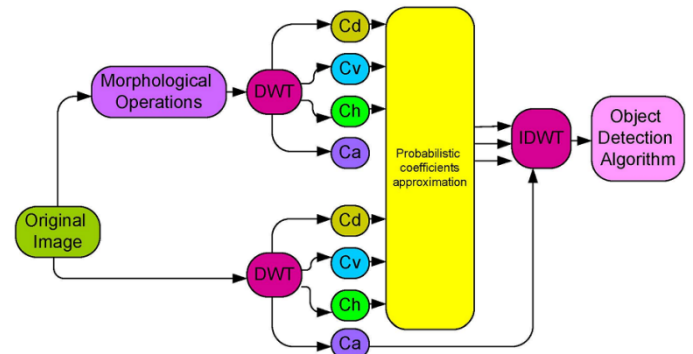


Figure 5. The Novel scheme for deformable shape matching based on approximation of wavelet coefficients

TABLE I. MAP DECISION RULES FOR VARIOUS PROBABILITY DISTRIBUTIONS OF WAVELET COEFFICIENTS

$p_w(W) = \frac{3}{2\pi\sigma^2} \cdot \exp\left(-\frac{\sqrt{3}}{\sigma} \sqrt{w_1^2 + w_2^2}\right)$	$w_{1,O}^2 + w_{2,O}^2 \leq \frac{W_M}{W_O} (w_{1,M}^2 + w_{2,M}^2)$
$p_w(W) = K \cdot \exp\left(-\left[a\sqrt{w_1^2 + w_2^2} + b(w_1 + w_2)\right]\right)$	$\left[a\sqrt{w_{1,O}^2 + w_{2,O}^2} + b(w_{1,O} + w_{2,O})\right] \leq \frac{W_M}{W_O} \left[a\sqrt{w_{1,M}^2 + w_{2,M}^2} + b(w_{1,M} + w_{2,M})\right]$
$p_w(W) = \frac{3}{2\pi\sigma_1\sigma_2} \cdot \exp\left(-\sqrt{3} \sqrt{\left(\frac{w_1}{\sigma_1}\right)^2 + \left(\frac{w_2}{\sigma_2}\right)^2}\right)$	$w_{1,O}^2 + w_{2,O}^2 \leq \frac{W_M}{W_O} (w_{1,M}^2 + w_{2,M}^2)$
$p_w(W) = K \exp\left(-\left[\sqrt{c_1 w_1^2 + c_2 w_2^2} + c_3 w_1 + c_4 w_2 \right]\right)$	$\left[\sqrt{c_1 w_{1,O}^2 + c_2 w_{2,O}^2} + c_3 w_{1,O} + c_4 w_{2,O} \right] \leq \frac{W_M}{W_O} \left[\sqrt{c_1 w_{1,M}^2 + c_2 w_{2,M}^2} + c_3 w_{1,M} + c_4 w_{2,M} \right]$

Derivation of MAP Decision rule for Model 1

$$p_w (W) = \frac{3}{2\pi\sigma^2} \cdot \exp\left(-\frac{\sqrt{3}}{\sigma} \sqrt{w_1^2 + w_2^2}\right)$$

Probability distribution of wavelet coefficients of Model 1 [9] is depicted in Figure 6.

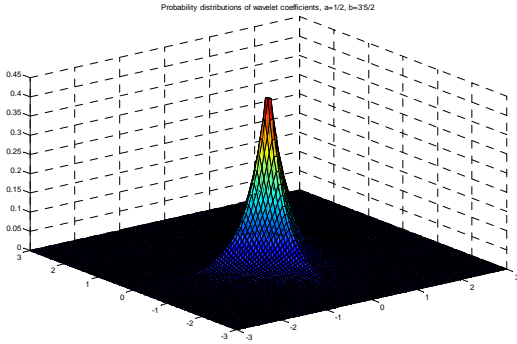


Figure 6. Probability distribution of wavelet coefficients, Model 1 [9]

$$p_{W, \text{Original}} (W_O) = \frac{3}{2\pi\sigma_O^2} \cdot \exp\left(-\frac{\sqrt{3}}{\sigma_O} \sqrt{w_{1,O}^2 + w_{2,O}^2}\right)$$

$$p_{W, \text{Morphology}} (W_M) = \frac{3}{2\pi\sigma_M^2} \cdot \exp\left(-\frac{\sqrt{3}}{\sigma_M} \sqrt{w_{1,M}^2 + w_{2,M}^2}\right)$$

$$\frac{\frac{3}{2\pi\sigma_O^2} \cdot \exp\left(-\frac{\sqrt{3}}{\sigma_O} \sqrt{w_{1,O}^2 + w_{2,O}^2}\right)}{\frac{3}{2\pi\sigma_M^2} \cdot \exp\left(-\frac{\sqrt{3}}{\sigma_M} \sqrt{w_{1,M}^2 + w_{2,M}^2}\right)} \begin{matrix} \text{Original} \\ \leq 1 \\ \text{Morphology} \end{matrix}$$

$$\exp\left(-\frac{\sqrt{3}}{\sigma_O} \sqrt{w_{1,O}^2 + w_{2,O}^2}\right) \leq \frac{W_O}{W_M} \frac{\sigma_O^2}{\sigma_M^2} \cdot \exp\left(-\frac{\sqrt{3}}{\sigma_M} \sqrt{w_{1,M}^2 + w_{2,M}^2}\right)$$

$$-\frac{\sqrt{3}}{\sigma_O} \sqrt{w_{1,O}^2 + w_{2,O}^2} \leq -\frac{\sqrt{3}}{\sigma_M} \sqrt{w_{1,M}^2 + w_{2,M}^2} + \ln \frac{\sigma_O^2}{\sigma_M^2}$$

$$\frac{\sigma_M}{\sigma_O} \sqrt{\frac{w_{1,O}^2 + w_{2,O}^2}{w_{1,M}^2 + w_{2,M}^2}} \leq 1 - \frac{\sqrt{3}}{3} \cdot \sigma_M \cdot \ln \frac{\sigma_O^2}{\sigma_M^2}$$

$$\sqrt{\frac{w_{1,O}^2 + w_{2,O}^2}{w_{1,M}^2 + w_{2,M}^2}} \leq \frac{W_M}{W_O} \frac{\sigma_O}{\sigma_M} \cdot \left(1 - \frac{\sqrt{3}}{3} \cdot \sigma_M \cdot \ln \frac{\sigma_O^2}{\sigma_M^2}\right)$$

$$w_{1,O}^2 + w_{2,O}^2 \leq \left(\frac{W_M}{W_O} \frac{\sigma_O}{\sigma_M} \cdot \left(1 - \frac{\sqrt{3}}{3} \cdot \sigma_M \cdot \ln \frac{\sigma_O^2}{\sigma_M^2}\right)\right)^2 (w_{1,M}^2 + w_{2,M}^2)$$

$$w_{1,O}^2 + w_{2,O}^2 \leq \frac{W_M}{W_O} (w_{1,M}^2 + w_{2,M}^2)$$

Derivation of MAP Decision rule for Model 2

$$p_w (W) = K \cdot \exp\left(-\left[a\sqrt{w_1^2 + w_2^2} + b(|w_1| + |w_2|)\right]\right)$$

Probability distribution of wavelet coefficients of Model 2 [9] is demonstrated in Figure 7-9 for various a and b.

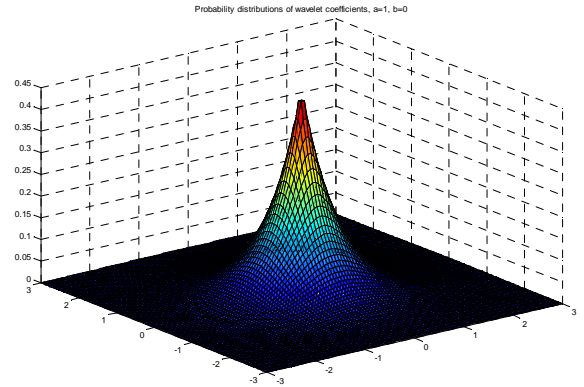


Figure 7. Probability distributions of wavelet coefficients, a=1, b=0

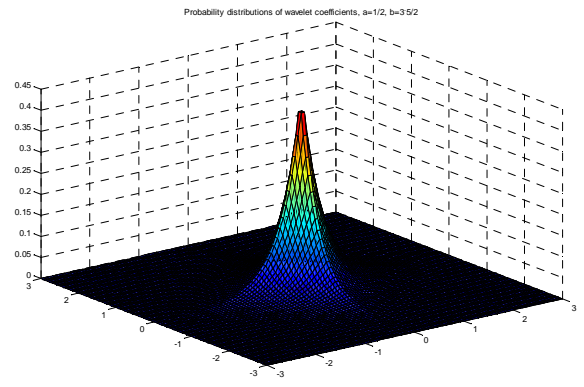


Figure 8. Probability distributions of wavelet coefficients, Model 2, a=1/2, b= $\frac{\sqrt{3}}{2}$

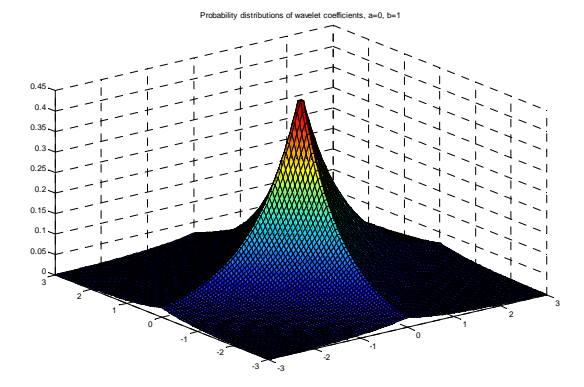


Figure 9. Probability distributions of wavelet coefficients, Model 2, a=0, b=1

$$p_{W, \text{Original}}(W_O) = K_O \cdot \exp\left(-\left[a_O \sqrt{w_{1,O}^2 + w_{2,O}^2} + b_O (|w_{1,O}| + |w_{2,O}|)\right]\right)$$

$$p_{W, \text{Morphology}}(W_M) = K_M \cdot \exp\left(-\left[a_M \sqrt{w_{1,M}^2 + w_{2,M}^2} + b_M (|w_{1,M}| + |w_{2,M}|)\right]\right)$$

$$\frac{K_O \cdot \exp\left(-\left[a_O \sqrt{w_{1,O}^2 + w_{2,O}^2} + b_O (|w_{1,O}| + |w_{2,O}|)\right]\right)}{K_M \cdot \exp\left(-\left[a_M \sqrt{w_{1,M}^2 + w_{2,M}^2} + b_M (|w_{1,M}| + |w_{2,M}|)\right]\right)} \leq 1$$

$$\exp\left(-\left[a_O \sqrt{w_{1,O}^2 + w_{2,O}^2} + b_O (|w_{1,O}| + |w_{2,O}|)\right]\right) \leq \frac{K_M}{K_O} \exp\left(-\left[a_M \sqrt{w_{1,M}^2 + w_{2,M}^2} + b_M (|w_{1,M}| + |w_{2,M}|)\right]\right)$$

$$-\left[a_O \sqrt{w_{1,O}^2 + w_{2,O}^2} + b_O (|w_{1,O}| + |w_{2,O}|)\right] \leq -\left[a_M \sqrt{w_{1,M}^2 + w_{2,M}^2} + b_M (|w_{1,M}| + |w_{2,M}|)\right] + \ln \frac{K_M}{K_O}$$

$$\left[a_O \sqrt{w_{1,O}^2 + w_{2,O}^2} + b_O (|w_{1,O}| + |w_{2,O}|)\right] \leq \left[a_M \sqrt{w_{1,M}^2 + w_{2,M}^2} + b_M (|w_{1,M}| + |w_{2,M}|)\right] - \ln \frac{K_M}{K_O}$$

$$\left[a \sqrt{w_{1,O}^2 + w_{2,O}^2} + b (|w_{1,O}| + |w_{2,O}|)\right] \leq \left[a \sqrt{w_{1,M}^2 + w_{2,M}^2} + b (|w_{1,M}| + |w_{2,M}|)\right]$$

Derivation of MAP Decision rule for Model 3

$$p_W(W) = \frac{3}{2\pi\sigma_1\sigma_2} \cdot \exp\left(-\sqrt{3} \sqrt{\left(\frac{w_1}{\sigma_1}\right)^2 + \left(\frac{w_2}{\sigma_2}\right)^2}\right)$$

A graph of probability distributions of wavelet coefficients, Model 3, [9] is shown in Figure 10.

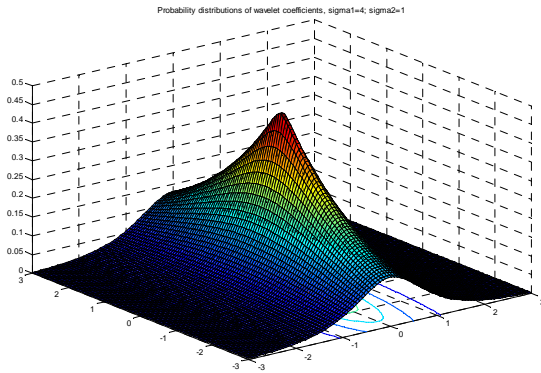


Figure 10. Probability distributions of wavelet coefficients, Model 3, $\sigma_1 = 4$, $\sigma_2 = 1$

$$p_{W, \text{Original}}(W_O) = \frac{3}{2\pi\sigma_{1,O}\sigma_{2,O}} \cdot \exp\left(-\sqrt{3} \sqrt{\frac{w_{1,O}^2}{\sigma_{1,O}^2} + \frac{w_{2,O}^2}{\sigma_{2,O}^2}}\right)$$

$$p_{W, \text{Morphology}}(W_M) = \frac{3}{2\pi\sigma_{1,M}\sigma_{2,M}} \cdot \exp\left(-\sqrt{3} \sqrt{\frac{w_{1,M}^2}{\sigma_{1,M}^2} + \frac{w_{2,M}^2}{\sigma_{2,M}^2}}\right)$$

$$\frac{\frac{3}{2\pi\sigma_{1,O}\sigma_{2,O}} \cdot \exp\left(-\sqrt{3} \sqrt{\frac{w_{1,O}^2}{\sigma_{1,O}^2} + \frac{w_{2,O}^2}{\sigma_{2,O}^2}}\right)}{\frac{3}{2\pi\sigma_{1,M}\sigma_{2,M}} \cdot \exp\left(-\sqrt{3} \sqrt{\frac{w_{1,M}^2}{\sigma_{1,M}^2} + \frac{w_{2,M}^2}{\sigma_{2,M}^2}}\right)} \leq 1$$

$$\exp\left(-\sqrt{3} \sqrt{\frac{w_{1,O}^2}{\sigma_{1,O}^2} + \frac{w_{2,O}^2}{\sigma_{2,O}^2}}\right) \leq \frac{W_O}{W_M} \frac{\sigma_{1,M}\sigma_{2,M}}{\sigma_{1,O}\sigma_{2,O}} \exp\left(-\sqrt{3} \sqrt{\frac{w_{1,M}^2}{\sigma_{1,M}^2} + \frac{w_{2,M}^2}{\sigma_{2,M}^2}}\right)$$

$$-\sqrt{3} \sqrt{w_{1,O}^2 + w_{2,O}^2} \leq -\sqrt{3} \sqrt{w_{1,M}^2 + w_{2,M}^2} + \ln \frac{\sigma_{1,M}\sigma_{2,M}}{\sigma_{1,O}\sigma_{2,O}}$$

$$\sqrt{w_{1,O}^2 + w_{2,O}^2} \leq \sqrt{w_{1,M}^2 + w_{2,M}^2} - \frac{\sqrt{3}}{3} \ln \frac{\sigma_{1,M}\sigma_{2,M}}{\sigma_{1,O}\sigma_{2,O}}$$

Morphological operators have translation invariance, monotony, duality and idempotent [31].

$$w_{1,O}^2 + w_{2,O}^2 \leq w_{1,M}^2 + w_{2,M}^2$$

Derivation of MAP Decision rule for Model 4

$$p_W(W) = K \cdot \exp\left(-\left[\sqrt{c_1 w_1^2 + c_2 w_2^2} + c_3 |w_1| + c_4 |w_2|\right]\right)$$

Figures 11 and 12 present probability distributions of wavelet coefficients, Model 4 [9] for various c_1, c_2, c_3 and c_4 .

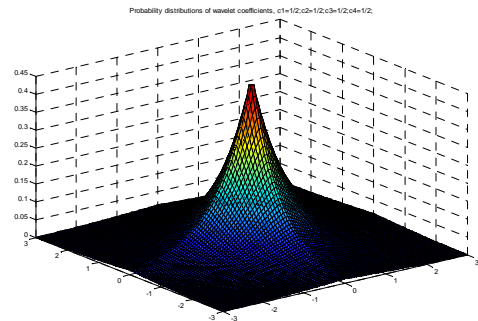


Figure 11. Probability distributions of wavelet coefficients, Model 4, [9] $c_1=1/2; c_2=1/2; c_3=1/2; c_4=1/2$;

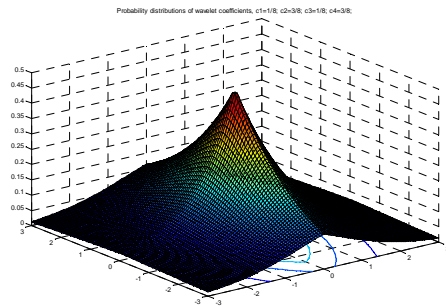


Figure 12. Probability distributions of wavelet coefficients, Model 4, $c_1=1/8; c_2=3/8; c_3=1/8; c_4=3/8$;

$$P_{W, \text{Original}}(W_O) = K_O \cdot \exp\left(-\left[\sqrt{c_{1,O} \cdot w_{1,O}^2 + c_{2,O} \cdot w_{2,O}^2 + c_{3,O} \cdot |w_{1,O}| + c_{4,O} \cdot |w_{2,O}|}\right]\right)$$

$$P_{W, \text{Morphology}}(W_M) = K_M \cdot \exp\left(-\left[\sqrt{c_{1,M} \cdot w_{1,M}^2 + c_{2,M} \cdot w_{2,M}^2 + c_{3,M} \cdot |w_{1,M}| + c_{4,M} \cdot |w_{2,M}|}\right]\right)$$

$$\frac{K_O \cdot \exp\left(-\left[\sqrt{c_{1,O} \cdot w_{1,O}^2 + c_{2,O} \cdot w_{2,O}^2 + c_{3,O} \cdot |w_{1,O}| + c_{4,O} \cdot |w_{2,O}|}\right]\right)}{K_M \cdot \exp\left(-\left[\sqrt{c_{1,M} \cdot w_{1,M}^2 + c_{2,M} \cdot w_{2,M}^2 + c_{3,M} \cdot |w_{1,M}| + c_{4,M} \cdot |w_{2,M}|}\right]\right)} \leq 1$$

$$\frac{W_O}{W_M} \leq \frac{K_M}{K_O} \exp\left(-\left[\sqrt{c_{1,O} \cdot w_{1,O}^2 + c_{2,O} \cdot w_{2,O}^2 + c_{3,O} \cdot |w_{1,O}| + c_{4,O} \cdot |w_{2,O}|}\right]\right)$$

$$\frac{W_O}{W_M} \leq \frac{K_M}{K_O} \exp\left(-\left[\sqrt{c_{1,M} \cdot w_{1,M}^2 + c_{2,M} \cdot w_{2,M}^2 + c_{3,M} \cdot |w_{1,M}| + c_{4,M} \cdot |w_{2,M}|}\right]\right) + \ln \frac{K_M}{K_O}$$

$$\frac{W_O}{W_M} \leq \frac{K_M}{K_O} \exp\left(-\left[\sqrt{c_{1,O} \cdot w_{1,O}^2 + c_{2,O} \cdot w_{2,O}^2 + c_{3,O} \cdot |w_{1,O}| + c_{4,O} \cdot |w_{2,O}|}\right]\right) - \ln \frac{K_M}{K_O}$$

$$\frac{W_O}{W_M} \leq \frac{K_M}{K_O} \exp\left(-\left[\sqrt{c_{1,O} \cdot w_{1,O}^2 + c_{2,O} \cdot w_{2,O}^2 + c_{3,O} \cdot |w_{1,O}| + c_{4,O} \cdot |w_{2,O}|}\right]\right) - \ln \frac{K_M}{K_O}$$

A typical scatter of two-component Gaussian mixture model is illustrated in Figure 13.

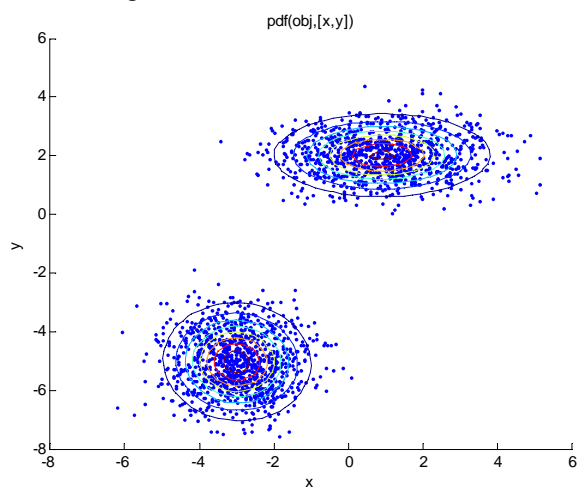


Figure 13. Typical scatter of two-component Gaussian mixture model.

IV. EXPERIMENTAL RESULTS

To evaluate the profit earning potential of this proposed pre-processing technique, the performance of an object detection method based on combination of AdaBoost learning with local histogram features [34 ,35] is compared in present and absence of this novel image enhancement technique.

Optimal adaptive mask can figure out more desired objects. Table II summarizes various experiments' results in the North American horses' image.

Experimental results of various morphological masking effects in circular object detecting with different radii in noisy and deformed image are compared in Figure 14. Their numerical results are summarized in Table III.

Experimental results show significantly improved performance is achieved using this approach in terms of detected shapes. Some of the results are depicted in Figure 15.

TABLE II. RESULTS OF VARIOUS EXPERIMENTS

Experiment	# Detected Horse	# undetected Horse
[I. Laptev, 2009, [34]]	17	32
[I. Laptev, 2009, [34]] with simple pre-processing	24	25
[I. Laptev, 2009, [34]] with optimal pre-processing	40	9

TABLE III. SUMMARIZED RESULTS OF SIMULATION COMPARISONS

	1st	2nd	3rd	4th	5th	6 th	Elapsed time
Novel	✓	✓	✓	✓	✓	✓	4.2
Gradient edge det.	✓	✓		✓		✓	5.6
Circular averaging	✓	✓	✓	✓	✓	✓	5.7
Prewitt	✓	✓		✓		✓	5.1
Sobel	✓	✓		✓		✓	5.4
Gaussian	✓	✓		✓	✓	✓	4.3
Average	✓	✓		✓	✓	✓	3.9
Center x	74	111	133	144	145	175	
Center y	197	78	136	205	117	164	
Radius	37	29	102	25	38	18	

V. CONCLUSION

This paper developed an object detection method of combining wavelet coefficients of both the original and morphologically filtered image. The novel method improves object recognition algorithms' performance by using better boundary detection. Results show that novel detection plan can achieve more accurate recognition performance. The paper achieves this improvement by applying an advanced pre-processing algorithm. However this advantage is obtained by increasing computational complexity which leads more requirements on processing capability of hardware and storage.

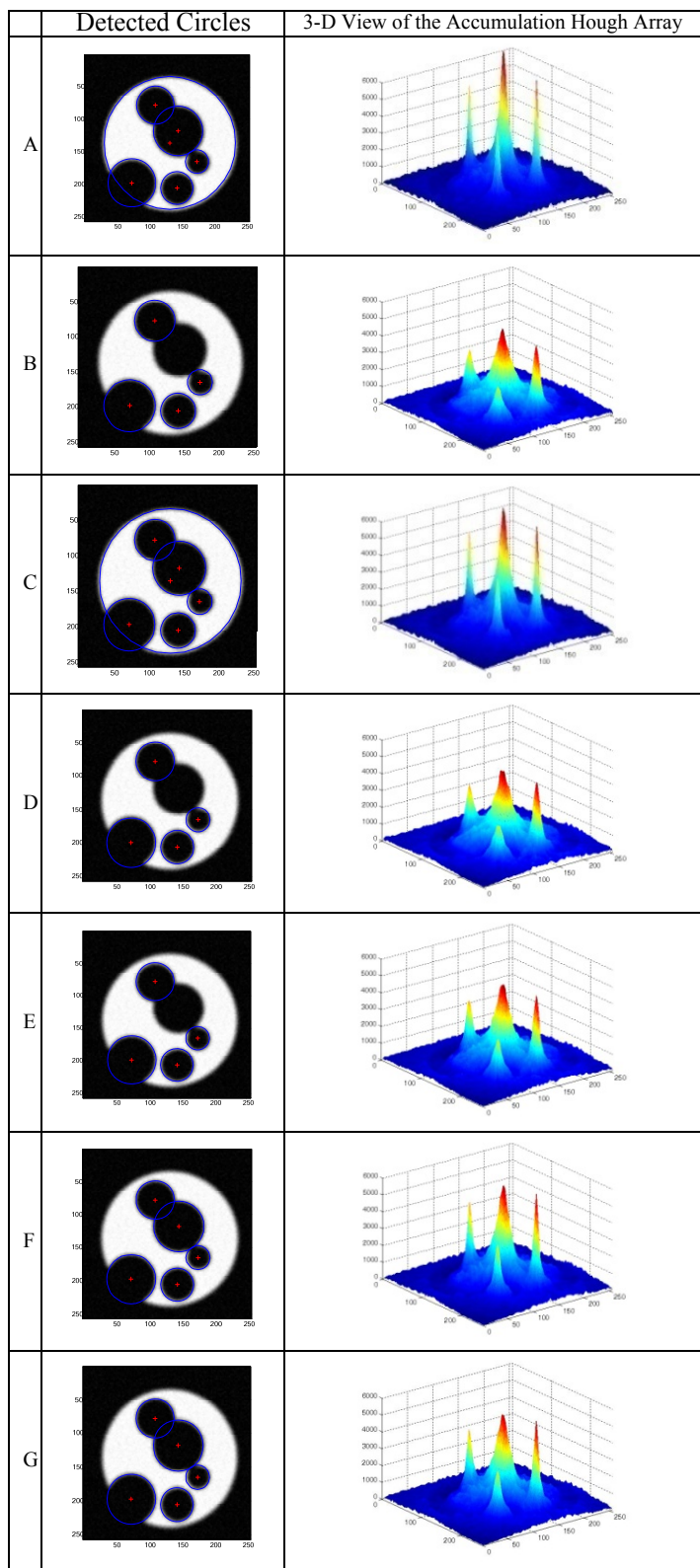


Figure 14. Detected circles and 3D view of the Hough accumulator of various convolution kernels for circular Hough transform, center positions and radii of detected circles are marked. A: Proposed mask, B: Reduced noise morphological edge detection, C: Circular averaging filter (kernel size 5×5), D: Prewitt horizontal edge emphasizing filter, E: Sobel horizontal edge-emphasizing filter, F: Gaussian lowpass filter $\sigma=1$ (kernel size 5×5), and G: Averaging filter (kernel size 3×3).

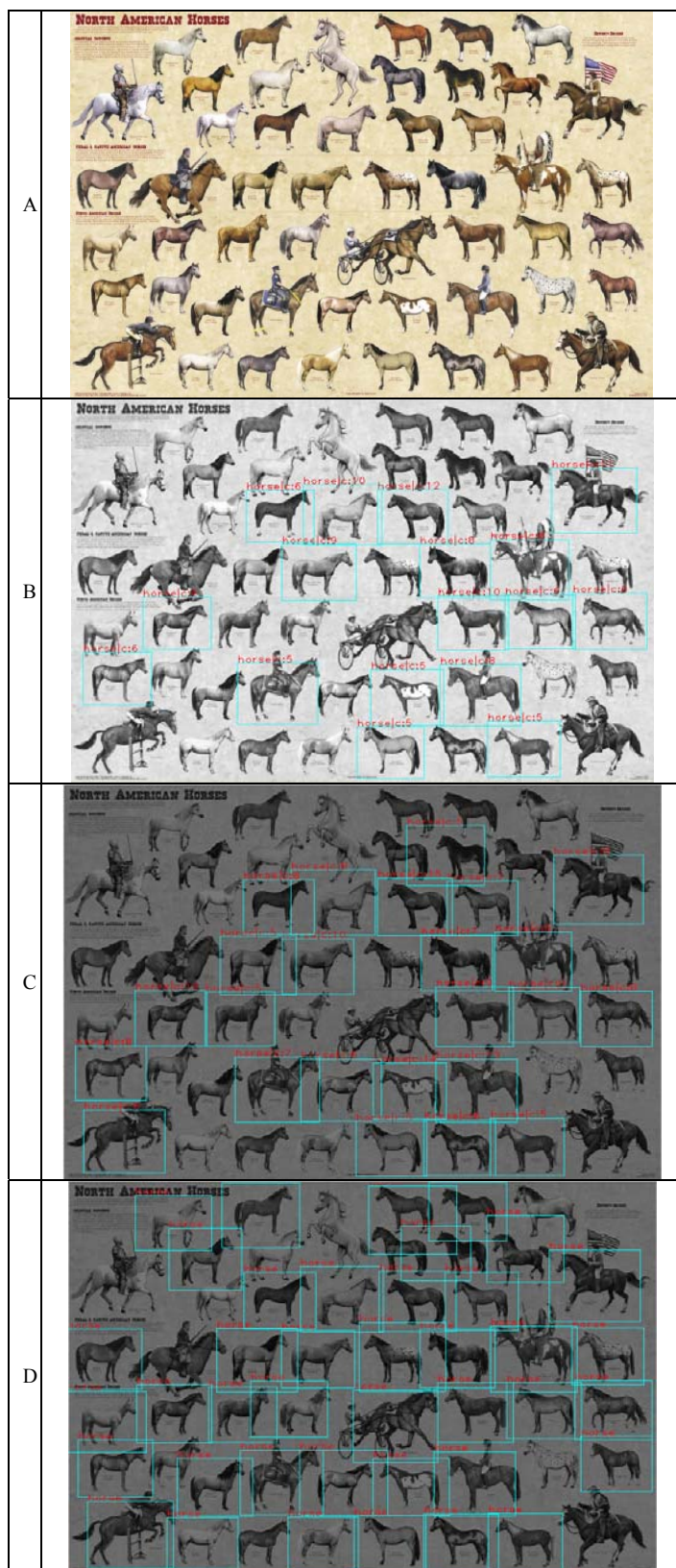


Figure 15. Experimental results of object detection algorithm in present and absence of proposed pre-processing scheme. A. original image, B. object detection results by [34], C. object detection results with simple considered pre-processing mask. D. object detection results with novel scheme pre-processing.

REFERENCES

- [1] J. Serra (1982): *Image Analysis and Mathematical Morphology*, Academic Press, London.
- [2] C. Guo, S. C. Zhu, and Y. N. Wu, "Primal sketch: Integrating structure and texture," *Comp. Vis. & Image Underst.*, 106, 5-19
- [3] Zhu Q., Payne M. and Riordan V. (1996). Edge linking by a directional potential functions, *Image & Vis.Comp.*14(1):59-70.
- [4] Elder J. H. and Zucker S.W. (1996). Computing contour closure, *Proceedings of the 4-th European Conference on Computer Vision- Volume I*, Cambridge, UK, 1, 399-412.
- [5] Chan T. F. and Vese L. A. (2001). Active contours without edges, *IEEE Transactions on Image Proc.* 10(2): 266-277.
- [6] Hyung II Koo; Nam IkCho , "Image de-noising based on a statistical model for wavelet coefficients", *Acoustics, Speech and Signal Processing*, 2008. ICASSP. IEEE International Conference on, March 31 -April 4 Page(s):1269 - 1272
- [7] Tan, Shan; Jiao, Licheng, "A unified iterative de-noising algorithm based on natural image statistical models: derivation and examples", *Optics Express*, 2008, vol. 16, issue 2, p. 975
- [8] AlexandruSar, SorinMoga, and DorinaSar, "A New De-noising System for SONAR Images", *EURASIP Journal on Image and Video Processing*, Volume 2009, Article ID 173841, 14 pages
- [9] L. Sendur and I. W. Selesnick, "Bivariate shrinkage with local variance estimation," *IEEE Signal Processing Letters*, vol. 9, no. 12, pp. 438-441, 2002.
- [10] A. Achim and E. E. Kuruolu, "Image de-noising using bivariate α -stable distributions in the complex wavelets domain," *IEEE Signal Processing Letters*, vol. 12, no. 1, pp. 17-20, 2005.
- [11] J. Portilla, V. Strela, M. J. Wainwright, and E. P. Simoncelli, "Image de-noising using scale mixtures of Gaussians in the wavelets domain," *IEEE Transactions on Image Processing*, vol. 12, no. 11, pp. 1338-1351, 2003.
- [12] A. Pizurica and W. Philips, "Estimating the probability of the presence of a signal of interest in multiresolution single- and multiband image de-noising," *IEEE Transactions on Image Processing*, vol. 15, no. 3, pp. 654-665, 2006.
- [13] E. P. Simoncelli and E. H. Adelson, "Noise removal via Bayesian wavelets coring," in *Proc. 3rd Int. Conf. on Image Processing (Lausanne, Switzerland, 1996)*, pp. 379-382.
- [14] S. G. Mallat, "A theory for multiresolution signal decomposition: the wavelets representation," *IEEE Pattern Anal. Machine Intell.*11, 674-693 (1989).
- [15] A. Achim, A. Bezerianos, and P. Tsakalides, "Novel Bayesian multiscale method for speckle removal in medical ultrasound images," *IEEE Trans. Med. Imag.*20, 772-783 (2001).
- [16] A. Achim, P. Tsakalides, A. Bezerianos, "SAR image de-noising via Bayesian wavelets shrinkage based on heavy-tailed modeling," *IEEE Trans. Geosci. Remote Sensing* 41, 1773-1784, 2001
- [17] J. Huang, "Statistics of natural images and models," PhD thesis, Division of Applied Mathematics, Brown University (2000).
- [18] U. Grenander A. Srivastava, "Probability models for clutter in natural images," *IEEE Pattern Anal. Machine Intell.*23, 424-429 (2001).
- [19] A. Srivastava, X. Liu, and U. Grenander, "Universal analytical forms for modeling image probability," *IEEE Pattern Anal. Machine Intell.*28, 1200-1214 (2002).
- [20] J. M. Fadili and L. Boubchir, "Analytical form for a Bayesian wavelets estimator of images using the Bessel K Form densities," *IEEE Trans. Image Processing* 14, 231-240 (2005).
- [21] B. Vidakovic, "Nonlinear wavelets shrinkage with Bayes rules and Bayes factors," *J. Amer. Stat. Assoc.* 93, 173-179 (1998).
- [22] H. A. Chipman, E. D. Kolaczyk, and R. E. McCulloch, "Adaptive Bayesian wavelets shrinkage," *J. Amer. Stat. Assoc.* 92, 1413-1421 (1997).
- [23] S. Tan and L. Jiao, "Wavelet-based Bayesian image estimation: from marginal and bivariate prior models to multivariate prior models," *IEEE Trans. Image Processing*, (2006).
- [24] T. A. Oigard, A. Hanssen, RE.Hansen, F. Godtliebsen, "EM-estimation and modeling of heavy-tailed processes with the multivariate normal inverse Gaussian distribution" *Signal Process.*85, 1655-1673 2005.
- [25] S. Tan and L. Jiao, "Multivariate statistical models for image de-noising in the wavelets domain," *International Journal of Computer Vision* 75, 209-230 (2007).
- [26] Shan Tan; Licheng Jiao; Kakadiaris, I.A., "Wavelet-Based Bayesian Image Estimation: From Marginal and Bivariate Prior Models to Multivariate Prior Models", *Image Processing, IEEE Transactions on*, Vol. 17, Issue 4, April 2008 Page(s):469 - 481
- [27] Lucio F. C. Pessoa, Petros Maragos : Neural networks with hybrid morphological/rank/linear nodes: a unifying framework with applications to handwritten character recognition, *PR*, 2000
- [28] Aishy Amer, "Binary Morphological operations for effective low-cost boundary detection", *Int. Journal of Pattern Recognition and Artificial Intelligence*, vol. 17, No. 2, March 2003, pp. 201-213.
- [29] P. Maragos, *Morphological Filtering for Image Enhancement and Feature Detection*, in *The Image and Video Processing Handbook*, Second Edition, edited by A. C. Bovik, Elsevier Acad. Press, 2005, pp.135-156.
- [30] Pengdong Xiao; Barnes, N.; Caetano, T.; Lieby, P.; An MRF and Gaussian Curvature Based Shape Representation for Shape Matching, *Computer Vision and Pattern Recognition*, 2007. CVPR '07. IEEE Conference on, 17-22 June 2007 Page(s):1 - 7
- [31] R. M. Haralick, S. R. Sternberg and X. Zhuang (1987) "Image Analysis Using Mathematical Morphology", *IEEE Transactions on Pattern Analysis and Machine Intelligence*, 9 (4): 532-550.
- [32] E. R. Dougherty and J. Astola (1994): *Introduction to Non-linear Image Processing*, SPIE, Bellingham, Washington.
- [33] Jun Yang and Xiaobo Li, *Boundary Detection Using Mathematical Morphology*, *Pattern Recognition Letters archive*. Volume 16 , Issue 12, December 1995, pp. 1287-1296.
- [34] I. Laptev, "Improving Object Detection with Boosted Histograms", in *Image and Vision Computing*, vol. 27, issue 5, pp. 535-544. 2009
- [35] I. Laptev, "Improvements of Object Detection Using Boosted Histograms"; in *Proc. BMVC'06*, Edinburgh, UK, pp. III:949-958, 2006